

Absorption of carbon dioxide into aqueous colloidal silica solution with different sizes of silica particles containing monoethanolamine

Byung-Jin Hwang*, Sang-Wook Park**†, Dae-Won Park*, Kwang-Joong Oh*, and Seong-Soo Kim**

*Division of Chemical Engineering, Pusan National University, Busan 609-735, Korea

**School of Environmental Science, Catholic University of Pusan, Busan 609-757, Korea

(Received 15 July 2008 • accepted 17 December 2008)

Abstract—Carbon dioxide was absorbed into an aqueous nanometer-sized colloidal silica solution in a flat-stirred vessel at 25 °C and 101.3 kPa to measure the absorption rate of CO₂. The concentrations of silica were in the range of 0-31 wt% and the sizes were 7, 60, and 111 nm. The solution contained monoethanolamine (MEA) of 0-2.0 kmol/m³. The volumetric liquid-side mass transfer coefficient ($k_L a$) of CO₂ was correlated with the empirical formula representing the rheological property of silica solution. The use of the aqueous colloidal silica solution resulted in a reduction of the absorption rate of CO₂ compared with Newtonian liquid based on the same viscosity of the solution. The chemical absorption rate of CO₂ was estimated by film theory using $k_L a$ and physicochemical properties of CO₂ and MEA.

Key words: Absorption, Carbon Dioxide, Silica, Viscoelastic Liquid, Monoethanolamine

INTRODUCTION

In multiphase systems appearing in agitated reactors, the gas-liquid mass transfer may be the rate-determining step for the overall process. For the reliable design of such reactors, therefore, a knowledge of the gas-liquid mass transfer rates characterized by the volumetric liquid-phase mass transfer coefficient ($k_L a$) is needed and many researchers [1] have studied how to enhance the mass transfer rate.

The dependence of shear stress on shear rate of a fluid in a hydrodynamic system is different according to the type of the fluid, i.e., Newtonian or non-Newtonian fluid, and the mass transfer coefficient (k_L) of a solute in one phase is in inverse proportion to the viscosity of its phase due to the inverse proportion of viscosity to diffusivity. The use of only the apparent viscosity of non-Newtonian fluids is not sufficient to obtain a unified correlation for $k_L a$. Due to the complexities of gas absorption in non-Newtonian media, the correlations obtained by these studies were limited to just a few kinds of non-Newtonian fluids.

If a considerable proportion of the reduction of $k_L a$ is due to the viscoelasticity of the aqueous solution [2,3], then the extent to which the data for a viscoelastic solution, such as polyacrylamide (PAA), deviate from those for an inelastic solution, such as carboxymethylcellulose (CMC), should be correlated with some measure of the solution's elasticity. The dimensionless Deborah number, De , which relates the elastic properties to the process parameters, is used to correlate $k_L a$ with the properties of non-Newtonian liquids. Unified correlations have been proposed for $k_L a$ in Newtonian as well as non-Newtonian solutions by introducing a dimensionless term, such as $(1+n_1 De^{n_2})^{n_3}$; they are listed in Table 1. As shown in Table 1, the values of the numbers in the dimensionless group are different from one another, and the polymers in Table 1 act as a reduction or in-

cremental agent in the absorption rate of the gas.

In slurry or colloidal systems, the effects of milli or micro particles on the absorption have been studied by many researchers [6-14]. The absorption of gas into slurries constituted by fine particles is a fairly common means of intensifying the gas absorption rates and even of improving selectivity in the case of multiple gaseous solutes. Improvement of the mass transfer rate by the use of the fine particles was explained by the mechanism of the grazing effect, first discovered by Kars and Best [6]. Zhou et al. [14] reviewed the effect of fine particles on multiphase mass transfer and concluded that the finer the particles in the slurries were, the stronger their influence was, and they reported that k_L might be increased or reduced via the variation of the film thickness caused by turbulence or the lowering of the diffusion coefficient of the gas. The reduction of the solubility and diffusivity of the dissolved gas in slurries with increasing volume fraction of the slurries may be due to the decrease [8] in the proportion of continuous phase in the slurries. As the volume fraction of the slurries is increased, the covering of the gas-liquid interface by fine particles can hinder the diffusion of the gas and, hence, reduce k_L .

In the recent decade, nanofluids have become one of the most attractive heat transfer media, due to the development of nano technology. A nanofluid is a solid/liquid mixture in which nano-sized particles ($d_p < 100$ nm) are suspended evenly in the base liquid. It is well known [15] that the use of a nanofluid can enhance the effective thermal conductivity and affect the heat transfer characteristic of fluid. If the nanofluid is treated as a pseudohomogeneous phase [12], in which the diffusion of the solutes and the gas-liquid interfacial area are assumed to be unaltered, the hydrodynamics of the nanofluid might be used to predict the gas absorption rate in the nanofluid/gas system. To the best of our knowledge, no studies have so far been conducted on the effect of a nanofluid on the mass transfer performance, although some researchers [16] have actively studied the enhancement of the heat transfer by using a nanofluid.

In our previous works [17-22], a series of works designed to in-

*To whom correspondence should be addressed.

E-mail: swpark@pusan.ac.kr

Table 1. Coefficients of dimensionless group for gas-liquid mass transfer correlation

Investigator	n ₁	n ₂	n ₃	Substance	Contactor
Nakanoh and Yoshida [3]	0.13	0.55	-1	CMC, PAA	Bubble column
Yagi and Yoshida [4]	2	0.5	-0.67	CMC, PA	agitated vessel
Ranade and Ulbrecht [5]	100	1	-0.67	CMC, PAA	stirred tank
Park et al. [17]	100	1	-0.42	PB, PIB	agitated vessel
Park et al. [18]	2461.3	1	-0.274	PB, PIB	agitated vessel
Park, et al. [19]	54.7	1	-0.45	PAA	agitated vessel
Park, et al. [20]	8.33	1.31	1	PEO	agitated vessel
Park, et al. [21]	0.5413	0.828	1	Xanthan gum	agitated vessel
Park, et al. [22]	9.4	1	-0.431	silica	agitated vessel

vestigate the effect that the behavior of a non-Newtonian liquid has on the gas absorption, we studied the effect of the elasticity of non-Newtonian liquid such as polyisobutylene (PIB) [17,18] in a benzene solution of polybutene (PB), PAA [19], polyethylene oxide (PEO) [20], and xanthan gum [21] on the absorption rate of CO₂ and correlated k_{la} with De as shown in Table 1. They presented the polymers used in their studies acting as accelerators or reducer of the absorption rate of CO₂ based on the same viscosity of the solution. Also, they measured k_{la} of CO₂ in an aqueous nano-sized solution of colloidal silica with a size of 24 nm [22] and correlated k_{la} with De as shown in Table 1. The value of k_{la} is influenced by the concentration of silica as shown in their work [22]. As a serial of their work [22], the effect of size of silica on k_{la} was investigated by using the nano-sized colloidal silica solutions with different sizes of silica in this study. Also, the chemical absorption rate of CO₂ by monoethanolamine (MEA) in aqueous colloidal silica solution was measured and analyzed by using k_{la}.

THEORY

The overall reaction between CO₂ (A) and MEA (B) in aqueous solution is



The overall chemical reaction of Eq. (1) is assumed to be second-order [23] as follows:

$$r_A = k_2 C_A C_B \quad (2)$$

Under the assumptions that MEA is a nonvolatile solute with its vapor pressure less than 0.2 mmHg at 20 °C, the gas phase resistance to absorption is negligible by using pure CO₂, and Raoult's law is applied, the mass balances of CO₂ and MEA, using film theory accompanied by chemical reactions, and the boundary conditions are given as follows:

$$D_A \frac{d^2 C_A}{dz^2} = k_2 C_A C_B \quad (3)$$

$$D_B \frac{d^2 C_B}{dz^2} = \nu k_2 C_A C_B \quad (4)$$

$$z=0, \quad C_A = C_{Ai}, \quad \frac{dC_A}{dz} = 0 \quad (5)$$

$$z=z_L, \quad C_A = 0, \quad C_B = C_{Bo} \quad (6)$$

The enhancement factor (β) by the chemical reaction is defined as the ratio of molar flux with a chemical reaction to that without a chemical reaction:

$$\beta = - \frac{D_A}{k_L C_{Ai}} \frac{dC_A}{dz} \Big|_{z=0} \quad (7)$$

Using β , the absorption rate (R_A) of CO₂ with a chemical reaction is estimated as follows:

$$R_A = \beta R_{Ao} = \beta k_{la} C_{Ai} V_L \quad (8)$$

where R_{Ao} is the physical absorption rate, which is obtained by multiplying the molar flux by the specific contact area between gas and liquid (a_l) and the liquid volume (V_L).

EXPERIMENTAL

1. Chemicals

All of the chemicals used in this study were of reagent grade and used without further purification. The purity of both CO₂ and N₂ was more than 99.9%.

Colloidal silica was synthesized according to the procedure reported elsewhere [24] using tetraethyl orthosilicate (Aldrich) as the silicon source and 25% aqueous ammonium hydroxide (Aldrich) to ensure the alkalinity of the reaction medium used as a catalyst, as follows:

Solution A: Tetraethyl orthosilicate (TEOS) of 30 ml was dissolved in ethyl alcohol of 325 ml. Solution B: Three volumes (5, 8, 12 ml) of aqueous ammonium hydroxide of 25% were dissolved in distilled water of 135 ml. Solution A and solution B were poured into the reactor with a mixer and a reflux condenser in a water bath and then the mixture was slowly stirred at 50 °C for 3 hours during which the clear liquid turned into a turbid gel. The solvent of this gel was removed in a vacuum evaporator below 50 °C to obtain solid particle of white color, which was dried in vacuum oven for 3 hours as colloidal silica.

Fig. 1 shows the surface pattern (SEM) of the synthesized colloidal silica. A uniform and spherical shape of SiO₂ are observable in the material and SEM illustrates average size of 17, 60, and 111 nm of the silica synthesized by NH₄OH of 5, 8, and 12 ml, respectively.

2. Absorption Rate of CO₂

An agitated semi-batch absorber used for measurement of the absorption rate of CO₂ was constructed of glass (0.102 m inside diameter; 0.151 m in height) with four equally spaced vertical baffles.

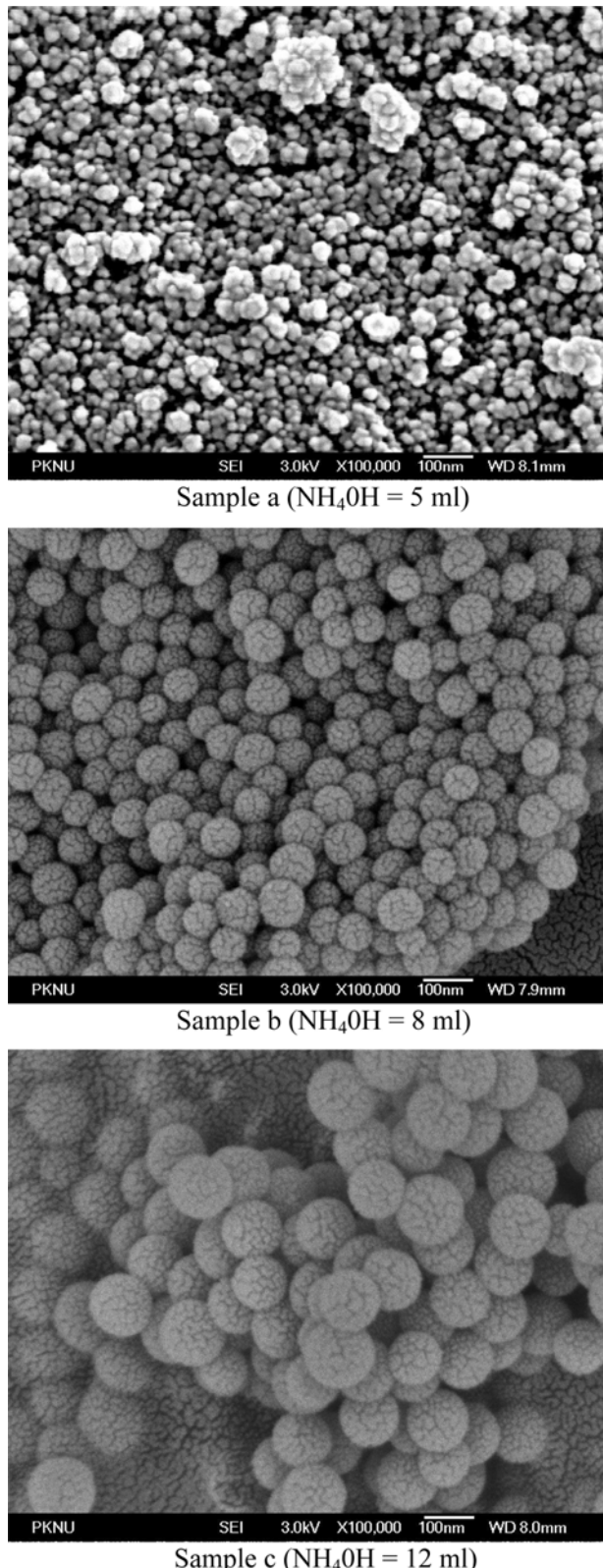


Fig. 1. SEM image patterns of the surface of silica particle (a: $d_p = 17$ nm, b: $d_p = 60$ nm, c: $d_p = 111$ nm).

A straight impeller with 0.05 m in length, 0.017 m in width, and 0.005 m in thickness was used as the liquid phase agitator, and was located at the middle position of the liquid phase of 0.3 dm³. The

effect of dead stagnant zones was assumed to be negligible by using the baffles. The contact area between gas and liquid was calculated from the ratio of the volume to the height of water added in the absorber, and its value was 43.2 cm². The absorption rates of CO₂ were measured by a procedure similar to that reported elsewhere [22] using a semi-batch absorber in the aqueous colloidal silica solution with silica concentration (C_s) in the range of 0-31 wt%, particle size (d_p) of 17, 60, and 111 nm, and MEA concentration (C_{Bo}) in the range of 0-2.0 kmol/m³ with an impeller speed of 50 rpm at 25 °C and 101.3 kPa.

PHYSICOCHEMICAL AND RHEOLOGICAL PROPERTIES

The physicochemical and rheological properties of the aqueous colloidal silica solution, which is assumed to be a nanofluid pseudo-homogeneous phase [12], were obtained as follows:

1. Physicochemical Properties of the Aqueous Colloidal Silica Solution

A pressure measuring method similar to the procedure reported elsewhere [25] was used, in which the pressure difference of CO₂ before and after equilibrium was achieved between the gas and liquid phase was measured to obtain the solubility (C_{Al}) of CO₂ in the aqueous colloidal silica solution at 25 °C and 101.3 kPa. The experimental procedure was described in detail in a previous publication [22]. The obtained values of C_{Al} for the various d_p and C_s values are given in Table 2.

The apparent viscosities (μ) of the aqueous colloidal silica solutions with various d_p and C_s values were measured with a Brookfield viscometer (Brookfield Eng. Lab. Inc, USA) and are given in Table 2.

D_A was correlated with the viscosity of the aqueous colloidal silica solution as follows:

$$D_A = D_{AW} \left(\frac{\mu_w}{\mu} \right)^{2/3} \quad (9)$$

since the experimental data [26] of the absorption rates are better correlated through the use of an index of 2/3 than 1. The diffusivities of CO₂ (D_{AW}) and MEA (D_{BW}) in water at 25 °C were taken to be 1.97×10^{-9} m²/s [27] and 1.1×10^{-9} m²/s [28], respectively. The diffusivity (D_B) of MEA in the aqueous colloidal silica solution was obtained from the assumption that the ratio of D_B to D_A was equal to the ratio in water [29].

The stoichiometric coefficient (ν) in Eq. (1) for MEA was obtained from the reference [23] and its value was 2.

The overall reaction rate constant (k₂) in the reaction of CO₂ with MEA was estimated as follows [23]:

$$\log k_2 = 10.99 - \frac{2152}{T} \quad (10)$$

2. Rheological Properties of the Aqueous Colloidal Silica Solution

We assumed that a power-law model, which has been widely used for the shear-dependent viscosity, can be used to represent the non-Newtonian flow behavior of the aqueous colloidal silica solution.

$$\tau = K\gamma^n \quad (11)$$

Table 2. Physicochemical and rheological properties of CO₂ and aqueous colloidal silica solution

d _p (nm)	C _s (wt%)	Viscosity (Ns/m ²) × 10 ³	Solubility (kmol/m ³)	Rheological properties				
				n	K × 10 ³ (Ns ⁿ /m ²)	b	A (Ns ⁿ /m ²)	De
17	0	0.890	0.039	1.00	1.00	0	0	0
	9.05	1.726	0.033	0.95	1.30	0.18	0.065	0.596
	18.27	2.878	0.029	0.89	1.61	0.21	0.094	0.774
	23.15	3.361	0.027	0.86	1.75	0.23	0.109	0.883
	30.63	3.986	0.026	0.81	2.01	0.25	0.131	1.003
60	0	0.894	0.039	1.00	1.00	0	0	0
	9.02	1.143	0.033	0.98	1.20	0.09	0.051	0.403
	18.17	1.612	0.029	0.95	1.37	0.11	0.073	0.537
	23.19	2.087	0.027	0.92	1.42	0.12	0.088	0.649
	30.51	2.954	0.026	0.87	1.51	0.13	0.104	0.757
111	0	0.894	0.039	1.00	1.00	0	0	0
	9.08	1.084	0.033	0.98	1.10	0.04	0.036	0.276
	18.63	1.318	0.029	0.96	1.22	0.07	0.052	0.389
	23.42	1.563	0.027	0.94	1.29	0.08	0.061	0.445
	30.46	1.948	0.026	0.91	1.38	0.09	0.078	0.553

$$\mu = K\gamma^{n-1} \quad (12)$$

$$N_i = A\gamma^b \quad (13)$$

where n, K, b, and A are material parameters depending on temperature. These parameters were obtained from the measurement of τ and N_i for the change of γ by a parallel disk type rheometer (Ares, Rheometrics, U.S.A.) with a diameter of 0.05 m and gap of 0.001 m.

The obtained values of n, K, b, and A for various values of d_p and C_s are given in Table 2. As shown in Table 2, the values of A increased with increasing C_s and decreasing d_p , which means that the aqueous colloidal silica solution exhibits elastic behavior [5].

One of the parameters used frequently to represent the characteristics of a material's viscoelasticity is known as the characteristic relaxation time (λ) of the liquid:

$$\lambda = \frac{N_i}{\mu\gamma^2} \quad (14)$$

Using Eqs. (12) and (13), λ is obtained as

$$\lambda = \frac{A}{K} \gamma^{b-n-1} \quad (15)$$

One of the dimensionless numbers, which relate the elastic properties with the process parameters, is the Deborah number (De). The characteristic flow time is measured against the characteristic process time (t), which is related to the reciprocal of the impeller speed (N) in the case of stirred tanks, and De is derived as follows:

$$De = \lambda/t = \frac{A}{K} \gamma^{b-n-1} N \quad (16)$$

where the shear rate (γ) is obtained in the case of the agitation of a liquid in a cylindrical vessel as follows [30]:

$$\gamma = 4\pi N h \quad (17)$$

The De values for various values of d_p and C_s at an agitation speed of 50 rpm in the absorber were calculated by using Eq. (15) and

May, 2009

are given in Table 2. As shown in Table 2, De increased with increasing C_s and decreasing d_p . This means that the finer the particles in the aqueous colloidal silica solution and the higher the concentration of silica, the stronger the influence of the elasticity.

RESULTS AND DISCUSSION

1. Empirical Correlation of Volumetric Liquid-side Mass Transfer Coefficient of CO₂

To observe the effect of d_p and C_s on the absorption rate (R_{A0}) and volumetric mass transfer coefficient ($k_L a$) of CO₂, R_{A0} was measured in the aqueous colloidal silica solutions of d_p of 17, 60, and 111 nm and C_s of 0-31 wt%, and then $k_L a$ was obtained from $R_{A0} =$

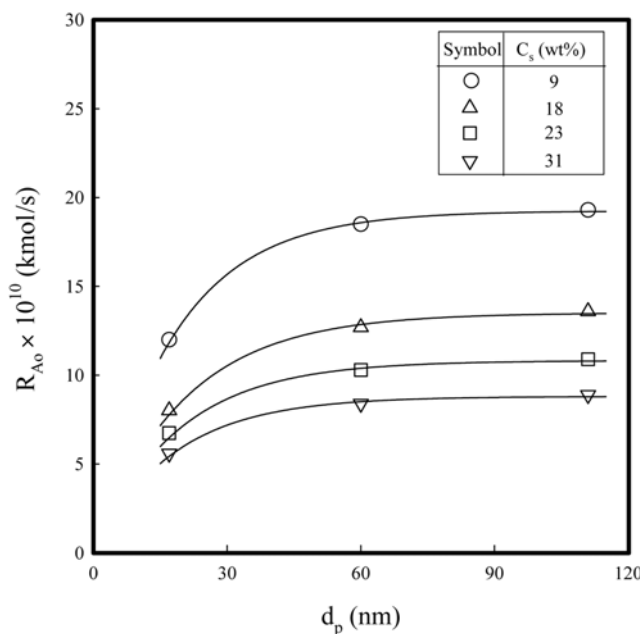
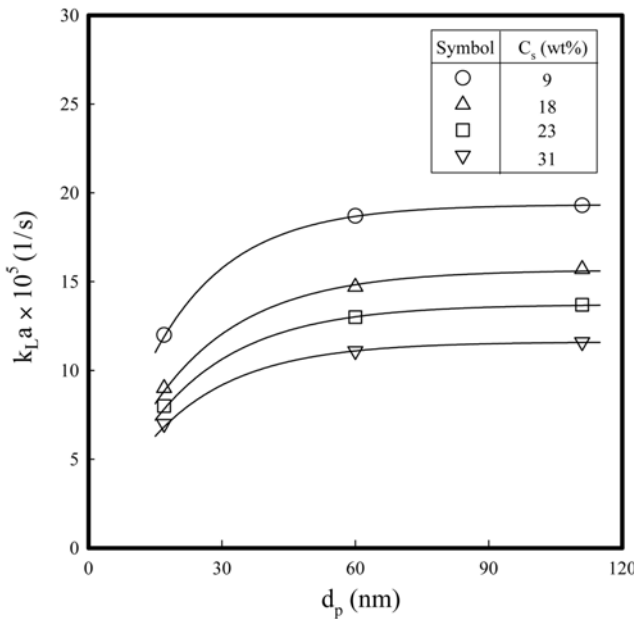


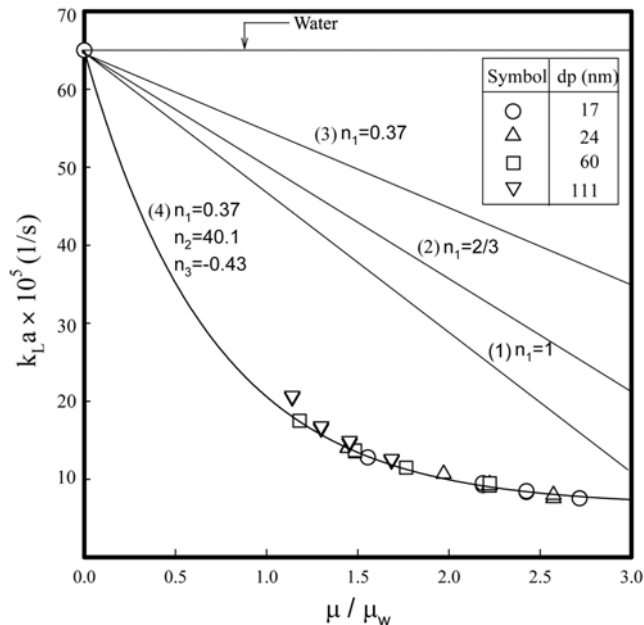
Fig. 2. R_{A0} vs. d_p for various C_s.

Fig. 3. $k_L a$ vs. d_p for various C_s .

$k_L a C_{Ai} V_L$. The values of R_{Ao} and $k_L a$ were plotted against d_p with the parameters of C_s in Figs. 2 and 3, respectively.

As shown in Figs. 2 and 3, R_{Ao} and $k_L a$ decrease with decreasing d_p and increasing C_s . Hikita et al. [8] measured the solubility and diffusivity of CO_2 in aqueous slurries of kaolin and explained that the reduction of the solubility and diffusivity of the dissolved gas in slurries with increasing volume fraction of the slurries caused by the increase in their concentration may be due to the decrease in the proportion of continuous phase in the slurries and the reduction of $k_L a$ due to the hindrance of the diffusion of the gas by the covered gas-liquid interface. The results in Figs. 2 and 3, which show that R_{Ao} and $k_L a$ decrease with increasing C_s , are the same as those reported in the paper [8], and may be due to the increase of the viscosity caused by the increase of C_s . On the other hand, at same C_s , the total volume fraction of silica should remain with increasing d_p and, hence, R_{Ao} and $k_L a$ may be the same despite the increase of d_p . However, R_A and $k_L a$ increased with increasing d_p , as shown in Figs. 2 and 3. This may be due to the decrease of the viscosity caused by the increase of d_p , as shown in Table 2. The solid lines in Figs. 2 and 3 were the calculated values of R_{Ao} and $k_L a$, respectively, which were obtained by using an empirical formula correlated with the rheological behavior of the solution and will be shown later.

It is customary to express the influence that the viscosity has upon k_L in terms of the Schmidt number (Sc), defined as $\mu/\rho D_A$, in which the viscosity is related to the diffusion coefficient. Instead of Sc, the ratio of viscosity of the solution to that of water was correlated with $k_L a$, as shown in the paper reported elsewhere [31], because the viscosity of the aqueous colloidal silica solution was related to d_p and C_s , and the viscosity in the agitated vessel depends on the rheological properties, as shown in Eq. (11) through Eq. (16). D_A is inversely proportional to μ in Stokes-Einstein equation, and k_L is directly proportional to D_A^n , where $n=1$ in the film theory, $1/2$ in the penetration model, and $2/3$ in relation between D_A and μ , as shown in Eq. (9).

Fig. 4. Coefficients of dimensionless group for $k_L a = k_{Lw} a (\mu_w/\mu)^{n_1} (1+n_2 De)^{n_3}$.

Based on the results mentioned above, we propose to correlate $k_L a$ in the aqueous colloidal silica solution with that in water as follows:

$$k_L a = k_{Lw} a \left(\frac{\mu_w}{\mu} \right)^{n_1} \quad (18)$$

The values of $k_L a$ are calculated from Eq. (18) against various values of d_p and C_s with n_1 of 1 and $2/3$, respectively, and plotted as solid lines 1 and 2 in Fig. 4. There were large differences between the measured $k_L a$ and calculated values with the standard deviation of 0.6005.

As shown in Fig. 4, there was a big difference between the calculated (lines 1 and 2) and measured values of $k_L a$ with correlation coefficients larger than 1; the correlation coefficient of line 1 with respect to the measured $k_L a$ is 5.297, and that of line 2 is 7.276. This means that the aqueous colloidal silica solution in this study does not follow the behavior of a Newtonian liquid.

Because the rheological properties of the aqueous colloidal silica solution were dependent on the viscoelasticity, as shown in Table 2, new terms corrected with the viscosity and De, in order to reduce the deviation of $k_L a$ for line 1 and 2 from the measured $k_L a$, were used as follows:

A simple multiple regression exercise using the viscosity and De in Table 2 was tried for the plots of $k_L a$ combined with the new terms such as $(\mu/\mu_w)^{n_1} (1+n_2 De)^{n_3}$ against the viscosity of the aqueous colloidal silica solution, which gave the values of n_1 , n_2 and n_3 . A multiple regression analysis provides the following correlation:

$$k_L a = k_{Lw} a \left(\frac{\mu_w}{\mu} \right)^{n_1} (1+n_2 De)^{n_3} \quad (19)$$

The values of $k_L a$ were calculated from Eq. (19) and shown as line 4 in Fig. 4 with values of n_1 of 0.37, n_2 of 40.1, and n_3 of -0.43 . As

shown in Fig. 4, the agreement between the measured values of $k_L a$ and those predicted by Eq. (19) is very good with a correlation coefficient of 0.998 and standard deviation of 0.0112.

The values of n_1 , n_2 , and n_3 in this study are the same as those ($n_1=0.37$, $n_2=39.4$, and $n_3=-0.43$) obtained by using a d_p value of 24 nm in the previous work [22]. That is, a Ludox HS-40 suspension (Aldrich) having a 40% w/w solid content (silica density of 2,200 kg/m³, specific surface area of 220 m²/g, PH of 9.8 as indicated by the manufacturer, Aldrich Chemical.) was used as colloidal silica with a particle size of 24 nm, De of the aqueous silica solution was measured with C_s in the range of 0-40.0 wt%, and $k_L a$ with impeller speed of 50-400 rpm, and impeller size of 0.034, 0.05, 0.075 m, respectively, at 25 °C and 101.3 kPa. The values of $k_L a$ obtained with these numbers using d_p of 24 nm were plotted with triangle symbol in Fig. 4. As shown in Fig. 4.1, the empirical formula of Eq. (19) can be applied to the case of d_p with 24 nm by fitting the triangle with Eq. (19).

It may be concluded that the exponent, m , in the relationship $k_L a \propto \mu^{-m}$ for stirred tanks is between 0.35 and 0.6 based on the previously reported values of m of 0.4 by Yagi and Yoshida [4], 0.41 by Ranade and Ulbrecht [5], and 0.38 by Moo-Young and Kawase [32]. The value of n_1 of 0.37 in this study compares well with the findings of the papers mentioned above. As a result in Fig. 4, the deviation of plots of $k_L a$ can be eliminated from solid line 3 to 4 by incorporating De into the correlation.

2. Effect of Rheological Properties on the $k_L a$ of CO_2

To observe the effect of viscoelasticity on $k_L a$, the value of $k_L a$ was obtained by using Eq. (19) with μ of the aqueous silica solution and De of 0 and plotted as solid line 3 in Fig. 4. The aqueous silica solution without elasticity (De=0) of line 3 is an imaginary solution, which is assumed to be a Newtonian liquid with the same viscosity as that of the aqueous silica solution with elasticity. As shown in Fig. 4, the value of $k_L a$ decreases in the following order: water line, line 3, line 4. In general, the mass transfer coefficient in the solution is inversely proportional to the viscosity. The viscosity of water is smaller than that of the aqueous silica solution, as listed in Table 2, and the value of $k_L a$ in water is larger than that in the aqueous silica solution. If the aqueous silica solution in this study only had viscous behavior, the value of $k_L a$ would be represented by line 3. However, the actual $k_L a$ of line 4 is smaller than that of line 3. The decrease of $k_L a$ from line 3 to line 4 might be due to the elasticity of the aqueous silica solution. In other words, the aqueous colloidal silica solution in this study might have the effect of reducing the value of $k_L a$ based on the same viscosity of the silica concentration.

3. Effect of Rheological Properties on the Chemical Absorption of CO_2

To observe the effect of viscoelasticity on the chemical absorption rate (R_A) of CO_2 into the aqueous MEA solution, R_A with and without silica was measured according to the change of C_{Bo} , d_p , and C_s .

Fig. 5 shows the plots of R_A against C_{Bo} using circles as the symbols in the range of 0-2.0 kmol/m³ under a typical d_p of 17 nm and C_s of 23 wt%. On the other hand, R_A was measured under the aqueous solution of MEA without silica, and plotted using triangles.

As shown in Fig. 5, R_A in the aqueous MEA solution with and without silica increase with increasing C_{Bo} , and R_A with silica is smaller than that without silica. Increase of R_A with increasing C_{Bo} is due to

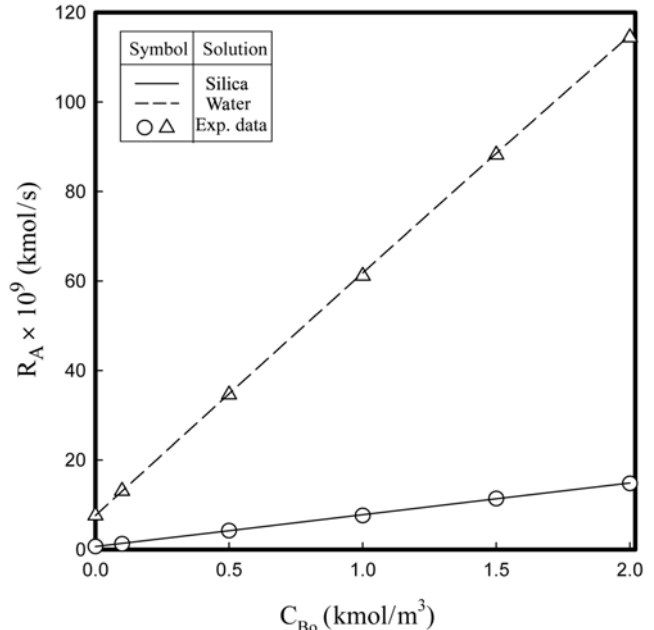


Fig. 5. R_A vs. C_{Bo} at $d_p=17$ nm and $C_s=23$ wt%.

the reactant of MEA in the chemical absorption of CO_2 , and the smaller R_A with silica than that without is due to the smaller $k_L a$ with than that without as shown in Eq. (19).

β is estimated by Eq. (7) and the numerical solution of Eq. (3), (4) by using the finite element method at given d_p , C_s , and C_{Bo} . R_A estimated from Eq. (8) under the same conditions as those in Fig. 5 was plotted with solid and dotted line symbols for the aqueous solution with and without silica, respectively. The calculated values of R_A are quite close to the measured values.

Fig. 6 shows the plots of R_A against C_s using circles as symbols in the range of 0-31 wt% under a typical d_p of 17 nm and C_{Bo} of

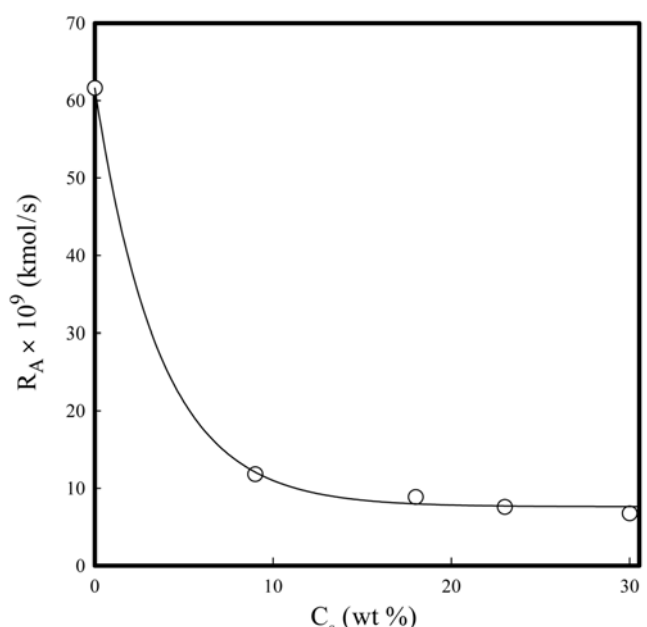


Fig. 6. R_A vs. C_s at $C_{Bo}=1$ kmol/m³ and $d_p=17$ nm.

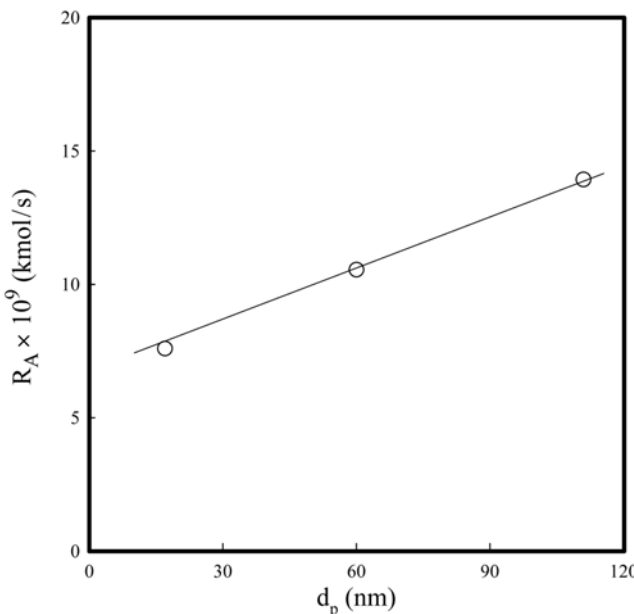


Fig. 7. R_A vs. d_p at $C_{Bo}=1 \text{ kmol/m}^3$ and $C_s=23 \text{ wt\%}$.

1.0 kmol/m³.

As shown in Fig. 6, R_A decreases with increasing C_s , which is due to the decrease of $k_L a$ caused by the increase of De through the increase of C_s as shown in Table 2 and Eq. (19).

Fig. 7 shows the plots of R_A against d_p using circles as the symbols in the range of 17-111 nm under a typical C_{Bo} of 1.0 kmol/m³ and C_s of 23 wt%.

As shown in Fig. 7, R_A increases with increasing d_p , which is due to the increase of $k_L a$ caused by the decrease of De through the increase of d_p as shown in Table 2 and Eq. (19).

CONCLUSIONS

The absorption rates of carbon dioxide in the aqueous colloidal silica solution were measured by using a flat-stirred vessel to observe the influence of the rheological properties of the aqueous colloidal silica solution on $k_L a$ under various experimental conditions: C_s in the range of 0-31 wt%, at d_p of 17, 60, and 111 nm, impeller size of 0.05 m, agitation speed of 50 rev/min 25 °C, and 101.3 kPa. The reduction effect of the elasticity of the aqueous colloidal silica solution on $k_L a$ was stronger than the effect of the viscosity, and $k_L a$ was correlated with an empirical formula representing the rheological behavior of the aqueous colloidal silica solution including the Deborah number as follows:

$$k_L a = k_{Lw} a \left(\frac{\mu_w}{\mu} \right)^{0.37} (1 + 40.1 De)^{-0.43}$$

The chemical absorption rate in the aqueous colloidal silica solution of MEA in the range of 0-2.0 kmol/m³ was estimated from the mass balance accompanied by chemical reaction based on film theory using the value of $k_L a$, and it was found that the reduction of $k_L a$ caused by the elastic properties of the aqueous colloidal silica solution causes a decrease of the chemical absorption rate of CO₂ at a given MEA concentration.

ACKNOWLEDGMENTS

This work was supported by THE Brain Korea 21 Project and a grant (2006-C-CD-11-P-03-0-000-2007) from the Energy Technology R&D of Korea Energy Management Corporation. Dae-Won Park is also thankful for KOSEF (R01-2007-000-10183-0).

NOMENCLATURE

a	: specific gas-liquid area [m^2/m^3]
C_i	: concentration of species, i [kmol/m^3]
d	: diameter of impeller [m]
d_p	: size of silica [nm]
D_i	: diffusivity of species, i [m^2/s]
De	: Deborah number
k_2	: reaction rate constant in reaction (1) [$\text{m}^3/\text{kmol}\cdot\text{s}$]
k_L	: liquid-side mass transfer coefficient of CO ₂ in absorbent [m/s]
$k_L a$: volumetric liquid-side mass transfer coefficient of CO ₂ in absorbent [1/s]
N_1	: primary normal stress difference [$\text{kg/m}\cdot\text{s}^2$]
V_L	: volume of the liquid phase [m^3]
r_A	: reaction rate in Equation (2) [$\text{kmol/m}^3\cdot\text{s}$]
R_A	: chemical absorption rate of CO ₂ [kmol/s]
R_{A0}	: physical absorption rate of CO ₂ [kmol/s]
T	: temperature [°K]
z	: diffusion coordinate of CO ₂ [m]
z_L	: film thickness [m]

Greek Letters

β	: enhancement factor of absorption rate by the chemical reaction
γ	: shear rate [1/s]
μ	: viscosity of silica solution [$\text{N}\cdot\text{s}/\text{m}^2$]
μ_w	: viscosity of water [$\text{N}\cdot\text{s}/\text{m}^2$]
ρ	: density of liquid [kg/m^3]
τ	: shear stress [N/m^2]

Subscripts

A	: CO ₂
B	: MEA
i	: gas-liquid interface
o	: bulk body of the liquid phase
s	: silica

REFERENCES

1. G. Astarita, D. W. Savage and A. Bisio, *Gas treatment with chemical solvents*, John Wiley & Sons, New York (1983).
2. G. Astarita, G. Greco Jr. and L. Nicodemo, *AIChE J.*, **15**, 564 (1969).
3. M. Nakanoh and F. Yoshida, *Ind. Eng. Chem. Process Des. Dev.*, **19**, 190 (1980).
4. H. Yagi and F. Yoshida, *Ind. Eng. Chem. Process Des. Dev.*, **14**, 488 (1975).
5. V. R. Ranade and J. J. Ulbrecht, *AIChE J.*, **24**, 796 (1978).
6. R. L. Kars and R. J. Best, *Chem. Eng. Sci.*, **17**, 201 (1979).
7. E. Sada, H. Kumazawa and C. H. Lee, *Chem. Eng. Sci.*, **39**, 117 (1984).

8. H. Hikita, K. Ishimi, K. Ueda and S. Koroyasu, *Ind. Eng. Chem. Process Des. Dev.*, **24**, 261 (1985).
9. G. Quicker, E. Alper and W. D. Deckwer, *AIChE J.*, **33**, 871 (1987).
10. A. Mehra, *Chem. Eng. Sci.*, **45**, 1525 (1990).
11. J. T. Tinge and A. A. H. Dringkenburg, *Chem. Eng. Sci.*, **50**, 937 (1995).
12. A. Mehra, *Chem. Eng. Sci.*, **51**, 461 (1995).
13. O. Ozkan, A. Calimli, R. Berber and H. Oguz, *Chem. Eng. Sci.*, **55**, 2723 (2000).
14. M. Zhou, W. F. Cai and C. J. Xu, *Korean J. Chem. Eng.*, **20**, 347 (2003).
15. P. Kebbinski, S. R. Phillipot, S. U. S. Choi and J. A. Eastman, *Int. J. Heat and Mass Transfer*, **45**, 855 (2002).
16. J. K. Kim, J. Y. Jung and Y. T. Kang, *Int. J. Refrigeration*, **29**, 22 (2006).
17. S. W. Park, I. J. Sohn, D. W. Park and K. J. Oh, *Sep. Sci. Technol.*, **38**, 1361 (2003).
18. S. W. Park, I. J. Sohn, S. G. Sohn and H. Kumazawa, *Sep. Sci. Technol.*, **38**, 3983 (2003).
19. S. W. Park, B. S. Choi, B. D. Lee and J. W. Lee, *Sep. Sci. Technol.*, **40**, 911 (2005).
20. S. W. Park, B. S. Choi and J. W. Lee, *Korean J. Chem. Eng.*, **24**, 431 (2007).
21. S. W. Park, B. S. Choi, K. W. Song, K. J. Oh and J. W. Lee, *Sep. Sci. Technol.*, **42**, 3537 (2007).
22. S. W. Park, J. W. Lee, B. S. Choi and J. W. Lee, *Sep. Sci. Technol.*, **41**, 1661 (2006).
23. H. Hikita, S. Asai and S. Ikuno, *AIChE J.*, **25**, 793 (1979).
24. C. J. Brinker and G. W. Scherer, *Sol-gel science*, Academic Press, New York (1990).
25. M. L. Kennard and A. Meisen, *J. Chem. Eng. Data*, **29**, 309 (1984).
26. L. K. Daraiswany and M. M. Sharma, *Heterogeneous reaction: Analysis, example and reactor design*, John Wiley & Sons, New York (1984).
27. H. Hikita, S. Asai and T. Takatsuka, *Chem. Eng. J.*, **11**, 131 (1976).
28. P. V. Danckwerts and M. M. Sharma, *Chem. Eng.*, **44**, 244 (1966).
29. R. A. T. O. Nijsing, R. H. Hendriksz and H. Kramers, *Chem. Eng. Sci.*, **10**, 88 (1959).
30. A. B. Metzner and R. E. Otter, *AIChE J.*, **3**, 3 (1957).
31. O. C. Sandall and K. G. Patel, *Ind. Eng. Chem. Process Des. Dev.*, **9**, 139 (1970).
32. M. Moo-Young and Y. Kawase, *Can. J. Chem. Eng.*, **65**, 113 (1987).